DMD Fast Forward. Published on December 22, 2014 as DOI: 10.1124/dmd.114.061887
This article has not been copyedited and formatted. The final version may differ from this version.

The Allosteric Binding Sites of Sulfotransferase 1A1

Ian Cook, Ting Wang, Charles N. Falany and Thomas S. Leyh

Department of Microbiology and Immunology (IC, TW, and TSL), Albert Einstein College of Medicine, 1300 Morris Park Ave, Bronx, New York 10461-1926 and the Department of Pharmacology and Toxicology, University of Alabama School of Medicine at Birmingham, 160 University Boulevard, VH151, Birmingham, Al 35294-0019 (CNF).

DMD Fast Forward. Published on December 22, 2014 as DOI: 10.1124/dmd.114.061887
This article has not been copyedited and formatted. The final version may differ from this version.

Running Title: SULT1A1 Allosteric Binding Sites

Corresponding Author:

Thomas Leyh, Ph. D.

The Department of Microbiology and Immunology

Albert Einstein College of Medicine

1300 Morris Park Ave.

Bronx, New York 10461-1926

Phone: 718-430-2857

Fax: 718-430-8711

E-mail: tom.leyh@einstein.yu.edu

Numbers:

Text of pages: 24

Tables: 2

Figures: 7

References: 40

Words in Abstract: 228

Words in Introduction: 400

Words in Discussion: 695

Abbreviations:

MEF, mefenamic acid, 2-(2,3-dimethylanilino)benzoic acid; EGCG, epigallocatechin gallate, [(2R,3R)-5,7-dihydroxy-2-(3,4,5-trihydroxyphenyl)-3,4-dihydro-2H-chromen-3-yl] 3,4,5-trihydroxybenzoate; PAPS 3'-phosphoadenosine 5'-phosphosulfate; PAP, 3′, 5′-diphosphoadenosine.

Abstract

Human sulfotransferases (SULTs) comprise a small, thirteen-member enzyme family that regulates the activities of thousands of compounds – endogenous metabolites, drugs and other xenobiotics. SULTs transfer the sulfuryl-moiety (-SO_3) from a nucleotide donor, PAPS (3'-phosphoadenosine 5'-phosphosulfate), to the hydroxyls and primary amines of acceptors. SULT1A1, a progenitor of the family, has evolved to sulfonate compounds that are remarkably structurally diverse. SULT1A1, which is found in many tissues, it is the predominant SULT in liver, where it is a major component of phase II metabolism. Early work demonstrated that catechins and NSAIDs (nonsteriodal anti-inflamatory drugs) inhibit SULT1A1, and suggested that the inhibition was not competitive *versus* substrates. Here, the mechanism of inhibition of a single, high-affinity representative from each class (epigallocatechin gallate (EGCG) and mefenamic acid) is determined using initial-rate and equilibrium-binding studies. The findings reveal that the inhibitors bind at sites separate from those of substrates, and at saturation, turnover of the enzyme is reduced to a non-zero value. Further, the EGCG inhibition patterns suggest a molecular explanation for its isozyme specificity. Remarkably, the inhibitors bind at sites that are separate from one another, and binding at one site does not affect affinity at the other. For the first time, it is clear that SULT1A1 is allosterically regulated, and that it contains at least two, functionally distinct allosteric sites, each of which responds to a different class of compounds.

Introduction

Human cytosolic sulfotransferases (SULTs) regulate the activities of thousands of small biomolecules – endogenous metabolites, drugs and other xenobiotics – *via* transfer of the sulfuryl-moiety (-SO_3) from the nucleotide donor, PAPS (3-phosphoadenosine 5'-phosphosulfate), to the hydroxyls and primary amines of acceptors. Small molecule sulfonation regulates numerous nuclear- and G-protein-coupled receptors by weakening, often dramatically, the affinities of agonists and antagonists, including steroid- (Parker, 1999, Zhang et al., 1998, Bai et al., 2011), thyroid- (Visser, 1994), and peptide-hormones (Matsubayashi and Sakagami, 2006), catecholamines (Johnson et al., 1980), bile acids (Takahashi et al., 1990), and dopamine (Whittemore et al., 1985). The ability of SULTs to recognize and sulfonate the receptor-binding determinants in complex small molecule structures helps preserve normal functioning of the receptors by preventing the adventitious binding of xenobiotics. SULTs neutralize toxins and pro-toxins by preventing either their action (Edavana et al., 2011) or their activation (Glatt et al., 2001), and by substantially shortening their terminal half-lives (Adjei et al., 2008, Argiolas and Hedlund, 2001). Finally, there are many examples of compounds whose activities are "switched on" by sulfonation (Cook et al., 2009, Meisheri et al., 1988). Speaking generally, the modification is used in metabolism either to control chemistry, or as a switch to toggle a molecule between distinctly different functional states.

SULT1A1, the focus of the current study, has a remarkably broad substrate spectrum (Berger et al., 2011, Nowell and Falany, 2006), which allows it to scan, and selectively modify, the scores of endogenous metabolites and xenobiotics that pass through hepatocyte cytosols. The molecular basis of this selectivity is intimately linked to the structure and dynamics of an approximately 30-residue active-site cap that mediates ligand-ligand and ligand-protein

interactions (Cook et al., 2013b, Leyh et al., 2013, Cook et al., 2013c, Cook et al., 2013a). SULT1A1 is the most abundant SULT in adult human liver, where it is present in gram quantities (Riches et al., 2009), and is a major component of phase II metabolism.

Evolutionary pressures have shaped SULT1A1 to select specific substrates from complex mixtures of compounds. It stands to reason that such an enzyme would contain allosteric sites that allow it to better communicate with its environment; yet, this issue has received little attention in the SULT field (Hunts et al., 1985). A small but important body of literature has investigated SULT1A1 inhibition by catechins (Coughtrie and Johnston, 2001) and nonsteroidal anti-inflammatory drugs (NSAIDs) (Vietri et al., 2000). The inhibition patterns from these partial studies suggested that the compounds might inhibit allosterically. If so, their further study could segue into a deeper understanding of SULT regulation. In the current work, the complete mechanism of inhibition of a single representative from each class was determined, and their interactions were studied. They are indeed allosteres and, remarkably, they bind at separate, non-interacting sites. The therapeutic implications of these sites are discussed. For the first time, it is clear that in addition to its substrate binding sites, SULT1A1 harbors two separate, allosteric binding pockets.

Materials and Methods

The experimental materials and their sources are as follows: dithiothreitol (DTT), dimethylsulfoxide (DMSO), ethylenediaminetetraacetic acid (EDTA), imidazole, isopropyl-thio-β-D-galactopyranoside (IPTG), Luria broth (LB), lysozyme, mefemanic acid, β-mercaptoethanol (β-ME), *p*-nitrophenol (pNP), pepstatin A, Na_2HPO_4, and NaH_2PO_4 were obtained from Sigma. Ampicillin, HEPES, KCl, KOH, $MgCl_2$, NaCl, and phenylmethylsulfonyl fluoride (PMSF) were purchased from Fisher Scientific. Epigallocatechin gallate was obtained from Santa Cruz Biotechnology, Inc. Glutathione- and nickel-chelating resins were obtained from GE Healthcare. Competent *Escherichia coli* (BL21(DE3)) cell was purchased from Agilent Technologies. PAP, PAPS were synthesized in-house as previously described (Zhang et al., 1998, Sun and Leyh, 2010, Cook et al., 2012) and were ≥ 98% pure as assessed by anion-exchange HPLC.

Protein Purification. The human SULT1A1 DNA was codon-optimized for *E. coli* (MR. GENE, Germany) and inserted into a pGEX6 vector containing a His/GST/MBP triple-affinity tag (Cook et al., 2013a). The enzyme was expressed in *E.coli* BL21(DE3) and purified according to a published protocol (Sun and Leyh, 2010). Briefly, enzyme expression was induced with IPTG (0.50 mM) in LB medium at 16°C for 14 hrs. The cells were pelleted, resuspended in lysis buffer, sonicated and centrifuged. The supernatant was loaded onto a Chelating Sepharose Fast Flow column charged with Ni^{2+}. The enzyme was eluted with imidazole (10 mM) onto a Glutathione Sepharose column from which it was then eluted with glutathione (10 mM). The tag was cleaved from SULT1A1 using PreScission protease, and the enzyme and tag were separated using a glutathione resin. Finally, the protein was concentrated using a Millipore Ultrafiltration

Disc (Ultracel 10 kDa cut off) and the concentration was determined spectrophotometrically (ε_{280} = 54 mM^{-1} cm^{-1}) (Cook et al., 2013a). The enzyme was flash frozen and stored at -80 °C.

Equilibrium binding of allosteric inhibitors to SULT1A1. The binding of allosteric inhibitors to different enzyme forms (E, E·pNP, E·PAPS and E·PAPS·pNP) was monitored *via* ligand-induced change of the enzyme intrinsic fluorescence (λ_{ex} = 290 nm, λ_{em} = 345 nm). Ligands were titrated into a solution containing SULT1A1 (10 nM, dimer), $MgCl_2$ (5.0 mM), $NaPO_4$ (50 mM), pH 7.2, T = 25 ± 2 °C. Titrations were performed in duplicate. Data were averaged and least-squares fit using a model that assumes a single binding site *per* monomer (Sun and Leyh, 2010, Cook et al., 2012).

Initial-rate Inhibition Studies. The initial-rate studies associated with Figures 1 and 4 have either PAPS or pNP as the varied substrate, and in each case the complementary substrate is held fixed and saturating (see Figures and Legends for exact concentrations). In each case, a 4 x 5 concentration matrix (substrate x inhibitor) was used to define the inhibition pattern, and the substrate and inhibitor concentrations were varied in equal increments in double-reciprocal space from 0.2 – 5 x K_m or K_i. In the studies associated with Figures 6 and 7, both PAPS or pNP are fixed and saturating. To ensure that velocities were measured during the initial rate of reaction, less than 5% of concentration-limiting reactant consumed at the reaction endpoint was converted during the measurement in all cases. The buffer composition and conditions for all of the studies were as follows: $NaPO_4$ (50 mM), $MgCl_2$ (5.0 mM), pH 7.2, T = 25 ± 2 °C.

DMD Fast Forward. Published on December 22, 2014 as DOI: 10.1124/dmd.114.061887
This article has not been copyedited and formatted. The final version may differ from this version.

Reaction progress was monitored differently depending on which substrate was held fixed. When PAPS was fixed, reactions were monitored *via* the loss in absorbance at 405nm that occurs as pNP is converted to pNPS (ε_{405}^{pNP} =10,300 $\pm$ 200 M^{-1} cm^{-1}, $\varepsilon_{405}^{pNPS} \sim$ 0.0 M^{-1} cm^{-1}). The pNP extinction coefficient was determined in the buffer used in the current study ($NaPO_4$ (50 mM), $MgCl_2$ (5.0 mM), pH 7.2, T = 25 $\pm$ 2 °C). Controls revealed that the salts in this buffer did not influence the pNP extinction coefficient at pH values where pNP is fully deprotonated (pH > 9), and its coefficient is well established (Biggs, 1954, Bowers et al., 1980, Anwar, 1984). When the pNP concentration was fixed, reaction progress was monitored by measuring the transfer of ^{35}S from ^{35}S-PAPS (15 nCi/reaction) pNP. To do so, the reactions were quenched at defined time intervals with NaOH (0.10 M, final), neutralized with HCl, boiled for 1.0 min and centrifuged at 12,100 x g. The samples were spotted onto an anion exchange TLC plate, and the labeled reactants were separated (LiCl mobile phase, 0.90 M) and quantitated using a STORM imaging system. Rates were obtained by least-squares fitting of 4-point progress curves.

DMD Fast Forward. Published on December 22, 2014 as DOI: 10.1124/dmd.114.061887
This article has not been copyedited and formatted. The final version may differ from this version.

Results and Discussion

EGCG Inhibition of SULT1A1. Catechins are water soluble flavinols that comprise ~ 25% of the dry weight of green tea, and EGCG accounts for approximately half of the tea catechins (Sabhapondit et al., 2012). Previous work on the interactions of SULTs and dietary chemicals revealed that EGCG is a potent inhibitor of SULT1A1 (K_i = 42 nM). The mechanism of inhibition appeared to uncompetitive *vs* PAPS; inhibition *vs* acceptor was not investigated. Initial-rate studies of EGCG inhibition *vs* both PAPS and acceptor (para-nitrophenol, pNP) are presented in Fig 1A and B. Inhibition *vs* PAPS is fit well using an uncompetitive model, which assumes that EGCG binds only to the PAPS-bound forms of the enzyme. In contrast, inhibition *vs* acceptor is well fit using a pure non-competitive model, indicating that EGCG and acceptor bind at separate sites, and they do not influence one another's affinity for the enzyme. The initial-rate inhibition parameters are listed in Table 1. The mechanism of SULT2A1 is rapid-equilibrium random (Wang et al., 2014), and it has been argued based on conservation of structure, the equivalence of initial-rate and thermodynamic parameters, and the partial substrate inhibition that is commonly within the family, that other SULTs, including SULT1A1 (Gamage et al., 2003) have similar mechanisms. Isotope-exchange experiments have been interpreted in favor of an ordered mechanism for SULT1A1; however, these results are also consistent with a random-binding mechanism that includes a dead-end complex (Cook and Cleland, 1981), which is the case with SULT1A1 (Gamage et al., 2005). For these reasons, we assume that the binding mechanism of SULT1A1 is random.

While the inhibition studies are revealing, they leave several key mechanistic issues unresolved. For example, a parallel-line inhibition pattern (Fig 1A) indicates only that inhibitor binds significantly more tightly to the nucleotide-bound than non-bound forms of the enzyme.

Further, the data do not address whether the enzyme is partially inhibited (i.e., turnover is reduced to a non-zero value at saturating inhibitor) or totally inhibited by EGCG.

To identify the enzyme forms to which EGCG binds and obtain its binding affinities, equilibrium-binding studies were performed using the enzyme forms typically associated with the substrate section of the catalytic cycle (E, E·pNP, E·PAPS, and E·pNP·PAP). It should be noted that PAP is an excellent surrogate for PAPS in ternary-complex binding studies (Cook et al., 2013a). Binding was monitored *via* ligand-induced changes in the intrinsic fluorescence of SULT1A1(Cook et al., 2013a). In all cases, substrate-ligand concentrations were ≥ 15 x K_d (Cook et al., 2013a, Cook et al., 2013c). The titrations are shown in Fig 2, and the affinity constants are compiled in Table 2.

The studies reveal that EGCG binds to all four enzyme forms - the mechanism is depicted in Fig 3. Its affinities for nucleotide-bound forms are identical within error, as are its affinities for the nucleotide-free forms; however, EGCG binds 21-fold more tightly to the enzyme when nucleotide is bound. The 21-fold difference in affinity provides an important clue as to the molecular basis of the inhibition. SULTs harbor a conserved 30-residue active-site cap that is positioned over both the nucleotide- and acceptor-binding pockets. Nucleotide binding stabilizes the cap in a “closed” position that encapsulates the nucleotide and acceptor and forms a pore that sterically restricts access to the acceptor-binding site (Leyh et al., 2013, Wang et al., 2014, Cook et al., 2013c). The cap can isomerize into an open state when nucleotide is bound, and it is from the open position that nucleotide escapes. The equilibrium constant for this isomerization, K_{iso}, has been measured for SULT1A1 and it equals 21 in favor of the closed position (Cook et al., 2013c, Cook et al., 2013a). The fact that the value for the PAPS-induced enhancement in EGCG affinity and K_{iso} are the same strongly suggests that EGCG binding is linked to cap closure. It is

DMD Fast Forward. Published on December 22, 2014 as DOI: 10.1124/dmd.114.061887
This article has not been copyedited and formatted. The final version may differ from this version.

particularly interesting that previous studies demonstrate that EGCG exhibits high affinity for SULT1A1, but not 1A2 or 1A3 (Coughtrie and Johnston, 2001), which are closely related isozymes whose caps differ slightly from that of SULT1A1. These facts, when taken together, are consistent with a model in which the isozyme specificity of the EGCG is determined by its interactions, either direct or indirect, with the cap.

MEF Inhibition of SULT1A1. A broad-based study of NSAID inhibition of SULT1A1 revealed that MEF is particularly potent (IC_{50} = 20 nM, (Vietri et al., 2002)); however, the mechanism of its inhibition is not known. MEF inhibition of the initial rate of SULT1A1 turnover is plotted *vs* PAPS and pNP in Fig 4A and B. The velocities were determined in triplicate, averaged, and were fit well using a non-competitive model, which assumes that the binding of substrate and inhibitor are entirely independent. The resulting affinity constants are compiled in Table 2. The simplest interpretation of these findings is that MEF binds to all four substrate forms of the enzyme at a site that is separate from those of the substrate-binding sites, and that MEF binding is not influenced by bound substrates. A notable feature of such mechanisms is that such inhibition cannot be "overcome" by an accumulation of substrate caused by restricted metabolic flow at the point of inhibition. It is interesting to note that the fact that MEF inhibits turnover without altering substrate affinities suggests that it perturbs only protein elements that control chemistry. Deeper mechanistic work will test this linkage.

To confirm the implications of the initial-rate findings, MEF binding to same four enzyme forms used in the EGCG study was investigated in equilibrium-binding studies. Here again, binding was monitored *via* changes in SULT1A1 intrinsic fluorescence. The results of the

titration (Fig 5) are consistent with the predictions of the initial-rate study - MEF binds to all four forms (Fig 3) and has nearly the same affinity (~23 nM) for each complex (Table 2).

EGCG and MEF are Partial Inhibitors. Partial inhibitors reduce turnover of an enzyme to a fixed, non-zero value at saturating inhibitor concentrations. The preceding initial-rate experiments do not have the resolution needed to distinguish between partial and total inhibition in cases where turnover is reduced to less than ~ 10% of non-inhibited turnover. To address this issue, the initial-rate of pNPS synthesis was determined at EGCE and MEF concentrations that ranged as high as 110 x K_i (Fig 6). Velocities were determined in triplicate and averaged. The data were fit using a model that assumes a single inhibitor-binding site per subunit, and the best-fits are shown as solid lines passing through the datasets. Turnover clearly decreases to a non-zero value at saturating inhibitor; thus, EGCG and MEF are partial inhibitors. At saturating concentrations of MEF and EGCG, SULT1A1 turnover is reduced to 6 ± 1 and 12 ± 2 %, respectively, of their uninhibited values.

EGCG and MEF Bind at Separate, Non-Interacting Sites. The mechanisms of EGCG and MEF inhibition are similar in that they each bind to the four enzyme forms studied; however, the fact that their inhibition mechanism differ (that is, only EGCG exhibits enhanced affinity when PAPS is bound) suggested that they might bind at separate sites. If so, and if they operate independently (i.e., they do not influence one another's affinity, or influence on turnover) their effects on SULT1A1 turnover will be additive. If, on the other hand, they bind at the same site, or at separate sites that are interactive, the effects will be non-additive. To assess the additivity of their effects, the inhibitors were used in combination, and the results were compared to the predictions of same- and separate-site binding models. The study simultaneously varied inhibitor concentrations in equal K_d-increments based on the constants in Table 1. Assuming separate,

non-interacting sites, this design causes the distribution of the inhibitor-bound forms of the enzyme to shift from predominantly single- to double-inhibitor occupancy as the concentration increases from low to high K_d equivalents. As the shift occurs, deviations from simple additivity can be observed. The patterns predicted by separate non-interacting, and same-site binding models are shown, in Fig 7, in solid and dashed lines, respectively. The models were parameterized using the constants obtained from the single-inhibitor studies (Table 1). The same-site model poorly describes the data; the separate non-interacting site model provides an excellent fit. Thus, each inhibitor binds at a separate site, and their actions are largely independent.

Inhibition by two independent, partial inhibitors differs substantially from that of a single inhibitor. At an inhibitor concentration equal to its affinity constant, assuming the enzyme concentration is negligible, half of the enzyme will be inhibitor bound. This is also the case for the second inhibitor, since it binds independently. The fraction of the enzyme bound to both inhibitors is given by the product of the fraction-bound for the individual inhibitors - in this case, 0.25. Thus, one quarter of the total enzyme will be in each of the four possible forms: E, $E{\cdot}I_A$, $E{\cdot}I_B$ and $E{\cdot}I_A{\cdot}I_B$. Turnover is given by the sum of the fraction of enzyme in each state weighted by its turnover. Given EGCG and Mef each at its K_d, turnover will be 29 percent of the uninhibited enzyme, which is nearly one-half (0.52) of that predicted for EGCG alone. An important consequence of double partial-inhibition is that turnover of double-inhibitor-bound enzyme is given by the product of the fraction-turnover associated with each inhibitor. Individually, EGCG and Mef reduce turnover to 0.12 and 0.06 times the non-inhibited value, respectively; together, they reduce turnover to near zero, 0.0072.

The affinities of EGCG (34 nM) and MEF (27 nM) for SULT1A1 are well below their normal plasma concentrations. Unmodified EGCG achieves a peak concentration of ~ 300 nM (8.8 x K_i) following consumption of 400 mg of pure compound, and consumption of MEF (500 mg) results in a peak concentration of 28 μM (1000 x K_i). While inhibition studies have not yet been performed in humans, the plasma-concentrations of EGCG and MEF are sufficient to inhibit 1A1 *in vivo*. It is notable that studies that used human liver extracts determined that the IC_{50} of MEF for SULT1A1 is approximately 20 nM (Vietri et al., 2002, De Santi et al., 2000).

Therapeutic Relevance. As our society evolves toward greater drug dependency, predicting drug-drug or drug-xenobiotic interactions becomes increasingly complex. The drug regime of an average nursing-home resident in the United States includes routine administration of 8.3 drugs and an additional 3.2 drugs that are given *pro re nata* (Jones Al et al., 2009). The better we understand the interactions of these compounds with their cellular counterparts the more able we are to predict whether compounds will interact, and the consequences of those interactions.

The neutralization of toxins, which occurs in a variety of ways, is among the primary functions of SULT1A1. Consider, for example, its role in preventing acetaminophen-induced hepatotoxicity - the most prevalent over-the-counter drug-induced hepatotoxicity in the United States (Larson et al., 2005). Acetaminophen is sulfonated (~40 %) by SULT1A1, and glucuronidated (~60%) by UGT1A1 (Rogers et al., 1987). While the conjugated form is non-toxic, the unconjugated compound is oxidized in liver, primarily by CYP3A4 (Larson et al., 2005), to *N*-acetyl-p-benzoquinone, which is cytotoxic. As the catalytic capacity of the conjugating systems become overwhelmed, either by overdose or inhibition due to co-administered compound, fatal toxicity can ensue (Larson et al., 2005). Thus one should

carefully consider whether individuals taking acetaminophen are also consuming catechin-rich foods and liquids, and/or NSAIDs.

Sulfonation is a primary pathway for the activation of poly-aromatic procarcinogens. The sulfonated derivatives of these compounds are unstable and thus disproportionate (heterolytically) into sulfate and highly reactive, planar electrophiles that covalently attach to DNA. *sult*-gene knock-in and knock-out studies (Sachse et al., 2014), and work with SULT-specific inhibitors, demonstrate that DNA adduct formation decreases dramatically when only the 1A1 isoform is inhibited. In this connection, it is notable that prostate cancer is 5 – 10-fold more likely in individuals that express high, *verses* low, levels of SULT1A1 activity in serum (Nowell et al., 2004). On the basis of these and similar findings, it is often suggested that, depending on diet, the routine consumption of SULT1A1 inhibitors contributes to a reduced incidence of cancer (Pasche et al., 2014, Thorat and Cuzick, 2013).

Recent work has shown that 76 of the 1211 FDA-approved small molecule drugs are sulfonated by SULT 1A1, and an additional 136 have been shown, or are predicted to be SULT1A1 inhibitors (Cook et al., 2013c). In many instances, sulfonation inactivates these drugs by preventing them from binding to their target receptors, and it can dramatically shorten their terminal half-lives. The extent of sulfonation is idiosyncratic to both the compound and its cellular locale. In certain cases, UGTs (UDP-glucuronosyltransferases) compensate for lowered SULT activity by glucuronidating the moiety that would otherwise have been sulfonated (Kane et al., 1995). In many cases, SULT inhibition is expected to enhance the efficacy of a drug. In cases like propofol, where rapid inactivation by 1A1 is desirable for quickly bringing patients out of anesthesia (Vree et al., 1987), SULT1A1 inhibition is detrimental. Alternatively, using inhibition of SULT1A1 to substantially lengthen the half-life and efficacy of apomorphine could

lead to a more stable anti-Parkinson's therapeutic and a substantially reduction in the tremors associated with the disease (Calabresi et al., 2010).

Conclusions

The mechanisms of SULT1A1 inhibition by EGCG and MEF have been determined. Both of the compounds bind to each of the four enzyme forms normally associated with the substrate "half" of the catalytic cycle (E, E·PAPS, E·pNP, and E·PAP·pNP), and both are partial inhibitors – the enzyme turns over at a reduced rate when inhibitor is bound. The coincidence of the increase in affinity of EGCG caused by PAPS binding (21-fold) and the isomerization equilibrium constant for closure of the active-site cap when is nucleotide bound suggests that ECGC interacts, either directly or indirectly, with the cap in its closed configuration. The binding affinity of EGCG is independent of the acceptor, pNP. Unlike EGCG, the affinity of MEF is identical for all four enzyme forms – nucleotide has no effect. Remarkably, EGCG and MEF do not interact – they bind at separate sites and do not influence one another's affinity. Thus, SULT1A1 has at least two independent allosteric-binding sites in addition to its substrate-binding sites. SULT1A1 has been designed not only to recognize an extremely broad range of acceptor structures, but to have multiple, independent allosteric binding pockets that are themselves broad in specificity. It is plausible, if not likely, that these sites will also respond to endogenous metabolites, and that they form the basis of an as yet unexplored molecular circuitry that enables the enzyme to sense and respond to the complex environment of the cytosol.

Author Contributions

Participated in research design: Cook, Wang, Falany, and Leyh

Conducted experiments: Cook and Wang

Contributed new reagents or analytic tools: none

Performed data analysis: Cook, Wang, and Leyh

Wrote or contributed to the writing of the manuscript: Cook, Wang, and Leyh

References

Adjei, A. A., Gaedigk, A., Simon, S. D., Weinshilboum, R. M. & Leeder, J. S. (2008). Interindividual variability in acetaminophen sulfation by human fetal liver: implications for pharmacogenetic investigations of drug-induced birth defects. *Birth Defects Res A Clin Mol Teratol,* 82**,** 155-65.

Anwar, B. E. (1984). The Effect of pH Various Additives on Extinction Coefficients for p-Nitrophenol. *Journal of Chemical Society of Pakistan,* 1.6**,** 55-61.

Argiolas, A. & Hedlund, H. (2001). The pharmacology and clinical pharmacokinetics of apomorphine SL. *BJU Int,* 88 Suppl 3**,** 18-21.

Bai, Q., Xu, L., Kakiyama, G., Runge-Morris, M. A., Hylemon, P. B., Yin, L., Pandak, W. M. & Ren, S. (2011). Sulfation of 25-hydroxycholesterol by SULT2B1b decreases cellular lipids via the LXR/SREBP-1c signaling pathway in human aortic endothelial cells. *Atherosclerosis,* 214**,** 350-6.

Berger, I., Guttman, C., Amar, D., Zarivach, R. & Aharoni, A. (2011). The molecular basis for the broad substrate specificity of human sulfotransferase 1A1. *PLoS One,* 6**,** e26794.

Biggs, A. I. (1954). A Spectrophotometric Determination of the Dissociation Constants of p-Nitrophenol and Papaverine. *Transactions of the Faraday Society,* 50**,** 800-802.

Bowers, G. N., Jr., Mccomb, R. B., Christensen, R. G. & Schaffer, R. (1980). High-purity 4-nitrophenol: purification, characterization, and specifications for use as a spectrophotometric reference material. *Clinical chemistry,* 26**,** 724-9.

Calabresi, P., Di Filippo, M., Ghiglieri, V., Tambasco, N. & Picconi, B. (2010). Levodopa-induced dyskinesias in patients with Parkinson's disease: filling the bench-to-bedside gap. *Lancet Neurol,* 9**,** 1106-17.

Cook, I., Wang, T., Almo, S. C., Kim, J., Falany, C. N. & Leyh, T. S. (2013a). The gate that governs sulfotransferase selectivity. *Biochemistry,* 52**,** 415-24.

Cook, I., Wang, T., Almo, S. C., Kim, J., Falany, C. N. & Leyh, T. S. (2013b). Testing the Sulfotransferase Molecular Pore Hypothesis. *J Biol Chem,* 288**,** 8619-26.

Cook, I., Wang, T., Falany, C. N. & Leyh, T. S. (2012). A Nucleotide-Gated Molecular Pore Selects Sulfotransferase Substrates. *Biochemistry,* 51**,** 5674-83.

Cook, I., Wang, T., Falany, C. N. & Leyh, T. S. (2013c). High Accuracy In-Silico Sulfotransferase Models. *J Biol Chem,* 288**,** 34494-501.

Cook, I. T., Duniac-Dmuchowski, Z., Kocarek, T. A., Runge-Morris, M. & Falany, C. N. (2009). 24-Hydroxycholesterol Sulfation by Human Cytosolic Sulfotransferases: Formation of Monosulfates and Disulfates, Molecular Modeling, Sulfatase Sensitivity and Inhibition of LXR Activation. *Drug Metab Dispos,* 37**,** 2069-78.

Cook, P. F. & Cleland, W. W. (1981). Mechanistic deductions from isotope effects in multireactant enzyme mechanisms. *Biochemistry,* 20**,** 1790-6.

Coughtrie, M. W. & Johnston, L. E. (2001). Interactions between dietary chemicals and human sulfotransferases-molecular mechanisms and clinical significance. *Drug Metab Dispos,* 29**,** 522-8.

De Santi, C., Pietrabissa, A., Spisni, R., Mosca, F. & Pacifici, G. M. (2000). Sulphation of resveratrol, a natural product present in grapes and wine, in the human liver and duodenum. *Xenobiotica,* 30**,** 609-17.

Edavana, V., Yu, X., Dhakal, I., Williams, S., Ning, B., Cook, I., Caldwell, D., Falany, C. & Kadlubar, S. (2011). Sulfation of Fulvestrant by Human Liver Cytosols and Recombinant SULT1A1 and SULT1E1. *Pharmacogenomics and Personalized Medicine,* 1**,** 137-145.

Gamage, N. U., Duggleby, R. G., Barnett, A. C., Tresillian, M., Latham, C. F., Liyou, N. E., Mcmanus, M. E. & Martin, J. L. (2003). Structure of a human carcinogen-converting enzyme, SULT1A1. Structural and kinetic implications of substrate inhibition. *J Biol Chem,* 278**,** 7655-62.

Gamage, N. U., Tsvetanov, S., Duggleby, R. G., Mcmanus, M. E. & Martin, J. L. (2005). The structure of human SULT1A1 crystallized with estradiol. An insight into active site plasticity and substrate inhibition with multi-ring substrates. *J Biol Chem,* 280**,** 41482-6.

Glatt, H., Boeing, H., Engelke, C. E., Ma, L., Kuhlow, A., Pabel, U., Pomplun, D., Teubner, W. & Meinl, W. (2001). Human cytosolic sulphotransferases: genetics, characteristics, toxicological aspects. *Mutat Res,* 482**,** 27-40.

Hunts, J., Ueda, M., Ozawa, S., Abe, O., Pastan, I. & Shimizu, N. (1985). Hyperproduction and gene amplification of the epidermal growth factor receptor in squamous cell carcinomas. *Jpn J Cancer Res,* 76**,** 663-6.

Johnson, G. A., Baker, C. A. & Smith, R. T. (1980). Radioenzymatic assay of sulfate conjugates of catecholamines and DOPA in plasma. *Life Sci,* 26**,** 1591-8.

Jones Al, Dwyer Ll, Bercovitz Ar & Strahan Gw (2009). The National Nursing Home Survey: 2004 Overview. 13**,** 26.

Kane, R. E., Li, A. P. & Kaminski, D. R. (1995). Sulfation and glucuronidation of acetaminophen by human hepatocytes cultured on Matrigel and type 1 collagen reproduces conjugation in vivo. *Drug Metab Dispos,* 23**,** 303-7.

Larson, A. M., Polson, J., Fontana, R. J., Davern, T. J., Lalani, E., Hynan, L. S., Reisch, J. S., Schiødt, F. V., Ostapowicz, G., Shakil, A. O., Lee, W. M. & Group, A. L. F. S. (2005).

Acetaminophen-induced acute liver failure: results of a United States multicenter, prospective study. *Hepatology,* 42**,** 1364-72.

Leyh, T. S., Cook, I. & Wang, T. (2013). Structure, dynamics and selectivity in the sulfotransferase family. *Drug Metab Rev***,** 423-30.

Matsubayashi, Y. & Sakagami, Y. (2006). Peptide hormones in plants. *Annu Rev Plant Biol,* 57**,** 649-74.

Meisheri, K. D., Cipkus, L. A. & Taylor, C. J. (1988). Mechanism of action of minoxidil sulfate-induced vasodilation: a role for increased K+ permeability. *J Pharmacol Exp Ther,* 245**,** 751-60.

Nowell, S. & Falany, C. N. (2006). Pharmacogenetics of human cytosolic sulfotransferases. *Oncogene,* 25**,** 1673-8.

Nowell, S., Ratnasinghe, D. L., Ambrosone, C. B., Williams, S., Teague-Ross, T., Trimble, L., Runnels, G., Carrol, A., Green, B., Stone, A., Johnson, D., Greene, G., Kadlubar, F. F. & Lang, N. P. (2004). Association of SULT1A1 phenotype and genotype with prostate cancer risk in African-Americans and Caucasians. *Cancer Epidemiol Biomarkers Prev,* 13**,** 270-6.

Parker, C. R. (1999). Dehydroepiandrosterone and dehydroepiandrosterone sulfate production in the human adrenal during development and aging. *Steroids,* 64**,** 640-7.

Pasche, B., Wang, M., Pennison, M. & Jimenez, H. (2014). Prevention and treatment of cancer with aspirin: where do we stand? *Semin Oncol,* 41**,** 397-401.

Riches, Z., Stanley, E. L., Bloomer, J. C. & Coughtrie, M. W. (2009). Quantitative evaluation of the expression and activity of five major sulfotransferases (SULTs) in human tissues: the SULT "pie". *Drug Metab Dispos,* 37**,** 2255-61.

Rogers, S. M., Back, D. J., Stevenson, P. J., Grimmer, S. F. & Orme, M. L. (1987). Paracetamol interaction with oral contraceptive steroids: increased plasma concentrations of ethinyloestradiol. *Br J Clin Pharmacol,* 23**,** 721-5.

Sabhapondit, S., Karak, T., Bhuyan, L. P., Goswami, B. C. & Hazarika, M. (2012). Diversity of catechin in northeast Indian tea cultivars. *ScientificWorldJournal,* 2012**,** 485193.

Sachse, B., Meinl, W., Glatt, H. & Monien, B. H. (2014). The effect of knockout of sulfotransferases 1a1 and 1d1 and of transgenic human sulfotransferases 1A1/1A2 on the formation of DNA adducts from furfuryl alcohol in mouse models. *Carcinogenesis,* 35**,** 2339-45.

Sun, M. & Leyh, T. S. (2010). The human estrogen sulfotransferase: a half-site reactive enzyme. *Biochemistry,* 49**,** 4779-85.

Takahashi, A., Tanida, N., Kang, K., Umibe, S., Kawaura, A., Furukawa, K., Hikasa, Y., Satomi, M. & Shimoyama, T. (1990). Difference in enzymatic sulfation of bile acids between the mouse and rat. *Tokushima J Exp Med,* 37**,** 1-8.

Thorat, M. A. & Cuzick, J. (2013). Role of aspirin in cancer prevention. *Curr Oncol Rep,* 15**,** 533-40.

Vietri, M., De Santi, C., Pietrabissa, A., Mosca, F. & Pacifici, G. M. (2000). Inhibition of human liver phenol sulfotransferase by nonsteroidal anti-inflammatory drugs. *Eur J Clin Pharmacol,* 56**,** 81-7.

Vietri, M., Vaglini, F., Pietrabissa, A., Spisni, R., Mosca, F. & Pacifici, G. M. (2002). Sulfation of R(-)-apomorphine in the human liver and duodenum, and its inhibition by mefenamic acid, salicylic acid and quercetin. *Xenobiotica,* 32**,** 587-94.

Visser, T. J. (1994). Role of sulfation in thyroid hormone metabolism. *Chem Biol Interact,* 92**,** 293-303.

Vree, T. B., Baars, A. M. & De Grood, P. M. (1987). High-performance liquid chromatographic determination and preliminary pharmacokinetics of propofol and its metabolites in human plasma and urine. *J Chromatogr,* 417**,** 458-64.

Wang, T., Cook, I., Falany, C. N. & Leyh, T. S. (2014). Paradigms of Sulfotransferase Catalysis - The Mechanism of SULT2A1. *J Biol Chem***,** 26474-80.

Whittemore, R. M., Pearce, L. B. & Roth, J. A. (1985). Purification and kinetic characterization of a dopamine-sulfating form of phenol sulfotransferase from human brain. *Biochemistry,* 24**,** 2477-82.

Zhang, H., Varlamova, O., Vargas, F. M., Falany, C. N. & Leyh, T. S. (1998). Sulfuryl transfer: the catalytic mechanism of human estrogen sulfotransferase. *J Biol Chem,* 273**,** 10888-92.

Footnotes

The work was supported by the National Institutes of Health Grants [GM38953, GM106158].

DMD Fast Forward. Published on December 22, 2014 as DOI: 10.1124/dmd.114.061887
This article has not been copyedited and formatted. The final version may differ from this version.

Figure Legends

Figure 1. ***The Inhibition of SULT1A1 by EGCG.*** **Panel A.** *EGCG vs PAPS.* PAPS concentration was varied from 0.2 – 5 x K_m, and EGCG concentrations are given in the figure. Reactions were initiated by addition of pNP at saturation (30 µM, 20 x K_m), and reaction progress was monitored by following formation of ^{35}S-pNPS. Velocities were determined by least-squares fitting of 4-point progress curves. Less than 5% of the concentration-limiting substrate consumed at the reaction endpoint was converted during the measurement. Velocities were determined in duplicate, averaged, and the data were fit globally using an *un-competitive* model. The results of the fit are given by the solid lines passing through the data. **Panel B.** *EGCG vs pNP.* Reactions were initiated by addition of PAPS at saturation (10 µM, 625 x K_m), the pNP concentration varied from 0.2 – 5 x K_m, and the EGCG concentration is given in the figure. Reaction progress was monitored at 405 nm. Less than 5% of the concentration-limiting substrate consumed at the endpoint of the reaction was converted during the measurement. Each point represents the average of three independent determinations. The lines through the points represent the behavior predicted by a global fit using a *non-competitive* inhibition model. Reaction conditions for both panels were as follows: SULT1A1 (10 nM, dimer), $MgCl_2$ (5.0 mM), and $NaPO_4$ (50 mM), pH = 7.2, and T = 25 ± °C.

Figure 2. ***The Binding of EGCG to SULT1A1.*** Binding was monitored *via* ligand-induced changes in the intrinsic fluorescence of SULT1A1 (λ_{ex} = 295 nm, λ_{em} = 345 nm). Conditions were as follows: SULT1A1 (10 nM, dimer), PAP (0 or 10 µM, 33 x K_d), pNP (0 or 45 µM, 30 x K_d), $MgCl_2$ (5.0 mM), $NaPO_4$ (50 mM), pH 7.2, T = 25 ± 2 °C. Each point is the average of two

independent determinations. The line through the data represents a least-squares fit using a model that assumes a single binding site per subunit.

Figure 3. ***The Mechanism of SULT1A1 Inhibition*** **.** Inhibitor (EGCG or MEF) binds to each of the enzyme forms in the substrate portion of the catalytic cycle. Turnover (k_{cat}) for the inhibited and non-inhibited species are related by α.

Figure 4. ***The Inhibition of SULT1A1 by MEF*****. Panel A.** *MEF vs PAPS*. Protocols were nearly identical to those associated with Fig 1A and B. PAPS concentration was varied from 0.2 – 5 x K_m, and MEF concentrations are listed in the figure. Reactions were initiated by addition of pNP at saturation (30 µM, 20 x K_m), and reaction progress was monitored by following formation of ^{35}S-pNPS. Velocities, obtained by least-squares fitting of 4-point progress curves, were determined in duplicate, averaged, and the data were fit globally using a *non-competitive* model. The fitting results are given by lines passing through the data. **Panel B.** *MEF vs pNP*. Reactions were initiated by addition of PAPS at saturation (10 µM, 625 x K_m). The pNP concentration varied from 0.2 – 5 x K_m, and MEF concentrations are given in the figure. Reaction progress was monitored at 405 nm. Less than 5% of the concentration-limiting substrate consumed at the endpoint of the reaction was converted during the measurement. Each point represents the average of three independent determinations. The lines through the points represent the behavior predicted by a global fit using a *non-competitive* inhibition model. Reaction conditions for both panels are as follows: SULT1A1 (5.0 nM, dimer), $MgCl_2$ (5.0 mM), and $NaPO_4$ (50 mM), pH = 7.2, and T = 25 ± °C.

Figure 5. ***The Binding of MEF to SULT1A1.*** The protocol was virtually identical to that described in Fig 2. Binding was monitored *via* ligand-induced changes in the intrinsic fluorescence of SULT1A1 (λ_{ex} = 295 nm, λ_{em} = 345 nm). Each point is the average of two independent determinations. The line through the data represents a least-squares fit using a model that assumes a single binding site per subunit. Conditions were as follows: SULT1A1 (10 nM, dimer), PAP (0 or 10 µM, 33 x K_d), pNP (0 or 45 µM, 30 x K_d), $MgCl_2$ (5.0 mM), $NaPO_4$ (50 mM), pH 7.2, T = 25 ± 2 °C.

Figure 6. ***EGCG and MEF are Partial Inhibitors.*** Reaction progress was monitored at 405 nm. The conditions were as follows: SULT1A1 (1.0 nM, dimer), PAPS (10 µM, 625 x K_m), PnP (30 µM, 22 x K_m), $MgCl_2$ (5.0 mM), $NaPO_4$ (50 mM), pH 7.2, T = 25 ± 2 °C. Less than 5% of the substrate converted at the endpoint of the reaction was consumed during the rate measurements. Each point represents the average of three independent determinations. The lines through the points indicate the behavior predicted by a least-squares fit using a model that assumes a single binding site per subunit. K_i values in the model were fixed using constants in Table 1, and data were fit only for the maximum inhibition value. The best-fit, maximum inhibition values for EGCG and MEF were 88 ± 2 and 94 ± 1 %, respectively.

Figure 7. ***EGCG and MEF Bind at Separate and Non-Interacting Sites.*** The pattern of SULT1A1 inhibition by EGCG and MEF in combination was used to assess their binding independence. EGCG and MEF were added simultaneously in equal K_i-equivalents over a concentration range that (based on single-inhibitor studies) will causes the enzyme to transition from singly- to doubly-inhibitor bound. The curving solid lines are the predictions of a same-site

(dashed line) and independent-site (solid line) binding models that were parameterized using the constants in Table 1. The experimental data (black dots) is in strong agreement with the additive model. Reaction conditions: SULT1A1 (20 nM), PAPS (10 µM, 625 x K_m), pNP (36 µM, 22 x K_m), $MgCl_2$ (5.0 mM), and $NaPO_4$ (50 mM), pH 7.2, T = 25 ± 2°C. Reactions were monitored at 405 nm. Each point is the average of three independent trials.

DMD Fast Forward. Published on December 22, 2014 as DOI: 10.1124/dmd.114.061887
This article has not been copyedited and formatted. The final version may differ from this version.

Tables

Table 1. SULT1A1 Inhibition by EGCG and MEF

Ligand	K_i (nM)	K_m (μM)	k_{cat} (min^{-1})
EGCG	34 (2)[1]		13 (2)[2]
MEF	27 (1)		6.6 (1)[2]
pNP		1.6 (0.1)[3]	66 (4)[3]
PAPS		0.016 (0.001)[3]	

[1]Values in parentheses indicate one Std Dev. [2]k_{cat} at saturating inhibitor (Fig 6 and related text). [3]Values determined at [Inhibitor] = 0.

DMD Fast Forward. Published on December 22, 2014 as DOI: 10.1124/dmd.114.061887
This article has not been copyedited and formatted. The final version may differ from this version.

Table 2. Inhibitor Affinities for SULT1A1 Complexes

	Enzyme Complex			
	E	E·PAPS	E·pNP	E·PAP·pNP
Inhibitor	K_d (nM)			
EGCG	820 (50)[1]	38 (3)	790 (30)	35 (2)
MEF	22 (1)	25 (1)	24 (2)	25 (1)

[1]Values in parentheses indicate one standard deviation.

Figure 1.

A)

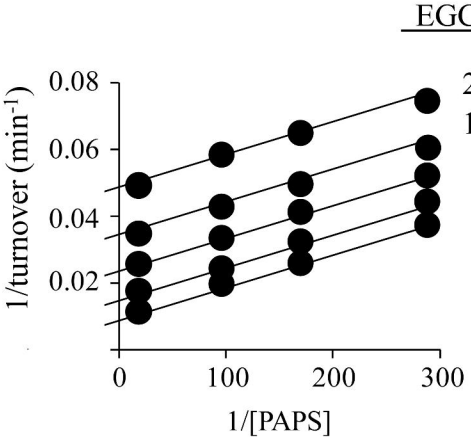
EGCG (nM)
200
130
60
20
0
0.08
0.06
0.04
0.02
1/turnover (min-1)
0
100
200
300
1/[PAPS]

B)

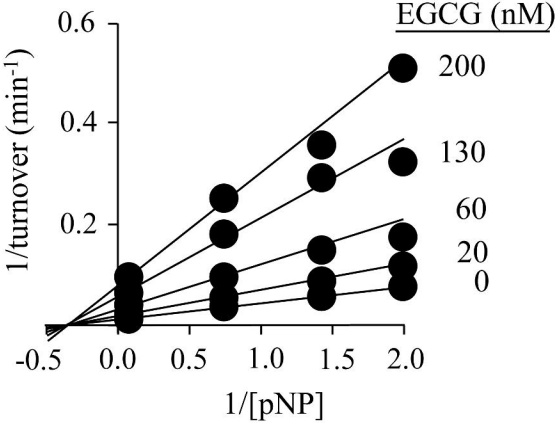
EGCG (nM)
200
130
60
20
0
0.6
0.4
0.2
1/turnover (min-1)
-0.5
0.0
0.5
1.0
1.5
2.0
1/[pNP]

Figure 2.

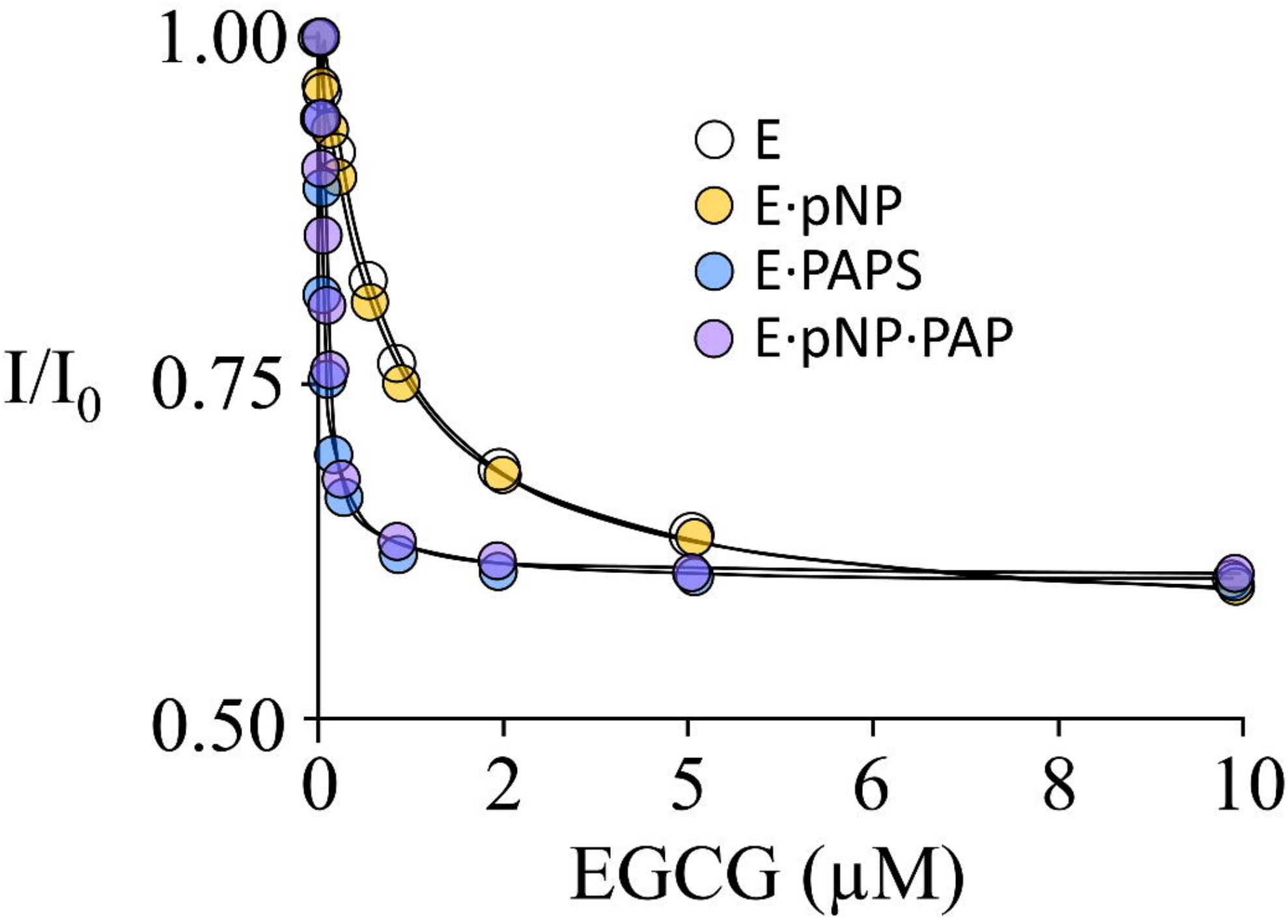

Figure 3.

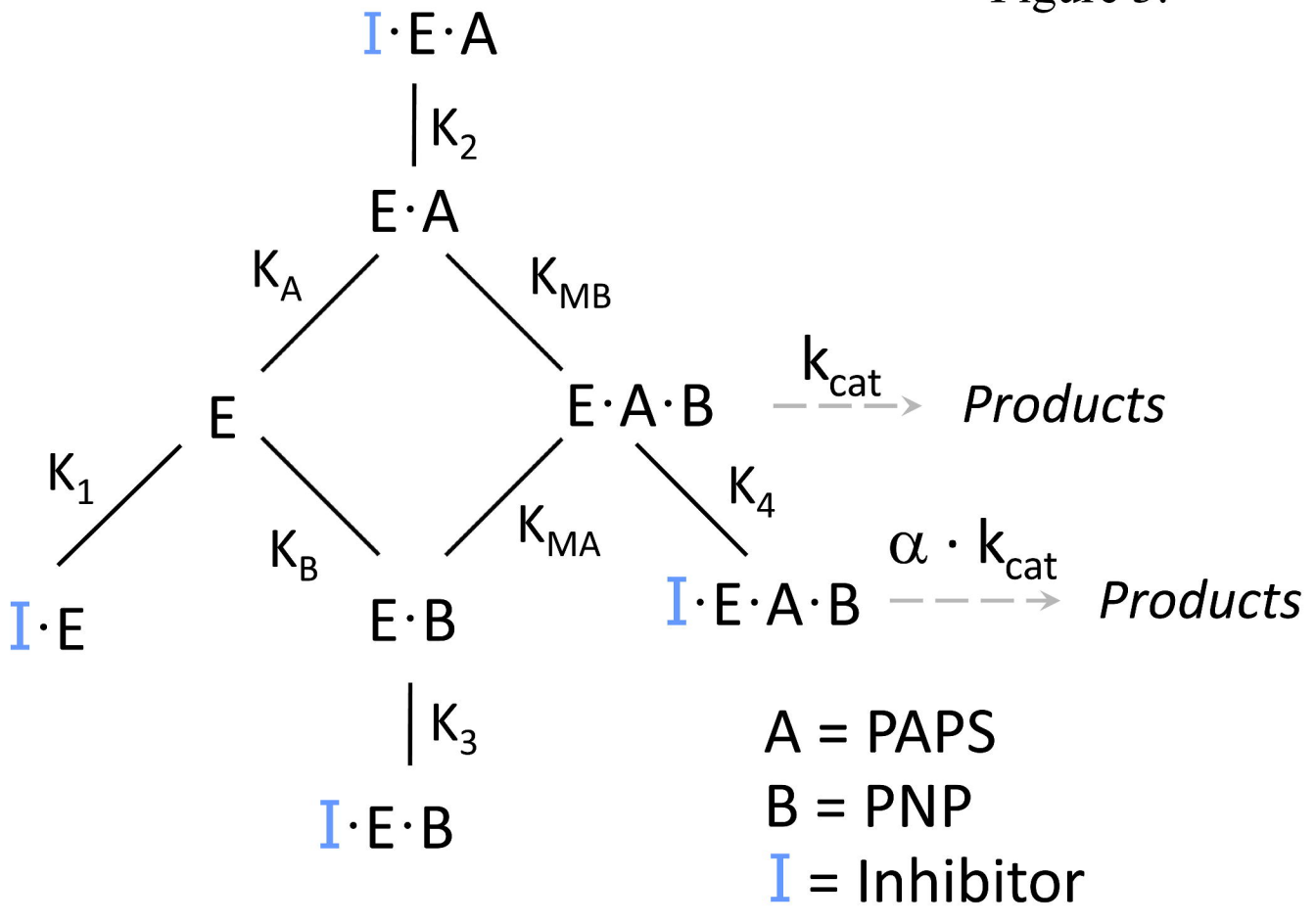
I·E·A
K2
E·A
KA
KMB
E
E·A·B
kcat
Products
K1
K4
KB
KMA
α · kcat
I·E
E·B
I·E·A·B
Products
K3
I·E·B
A = PAPS
B = PNP
I = Inhibitor

Figure 4.

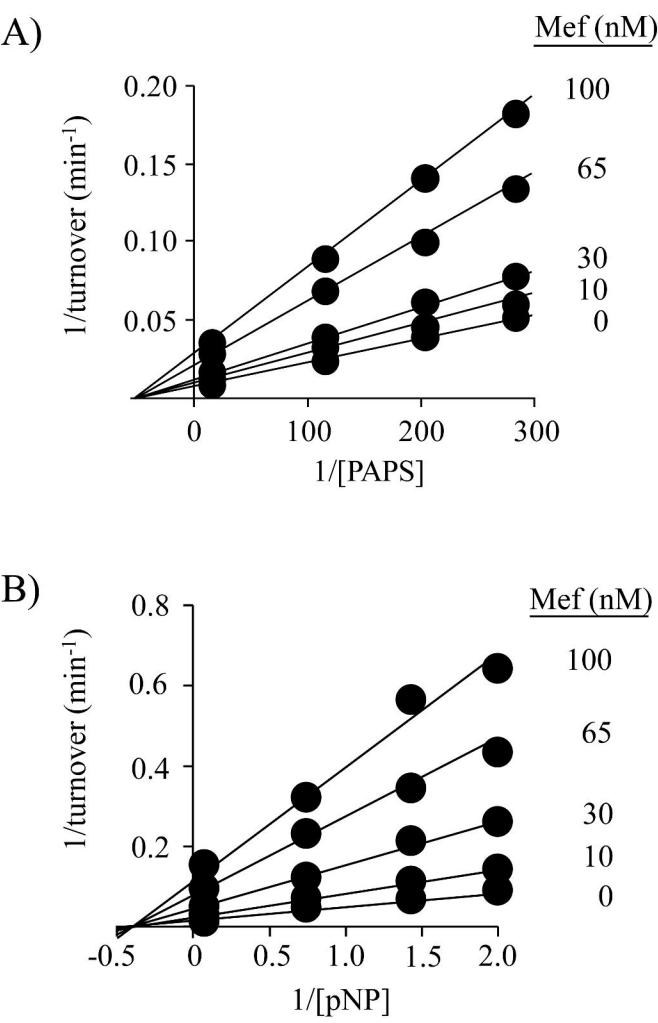
A)
Mef (nM)
100
65
30
10
0
0.20
0.15
0.10
0.05
1/turnover (min-1)
0
100
200
300
1/[PAPS]
B)
Mef (nM)
100
65
30
10
0
0.8
0.6
0.4
0.2
1/turnover (min-1)
-0.5
0
0.5
1.0
1.5
2.0
1/[pNP]

Figure 5.

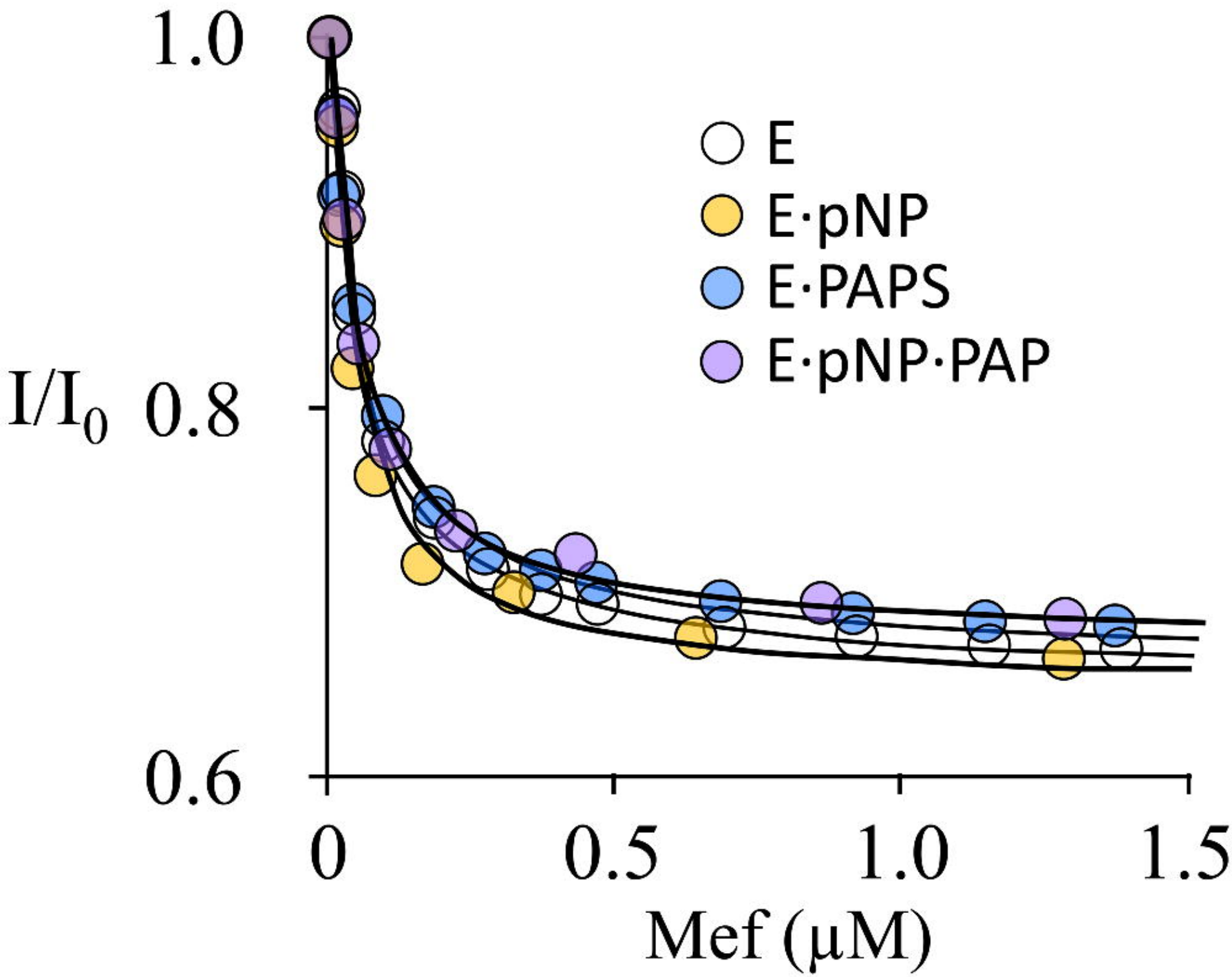

Figure 6.

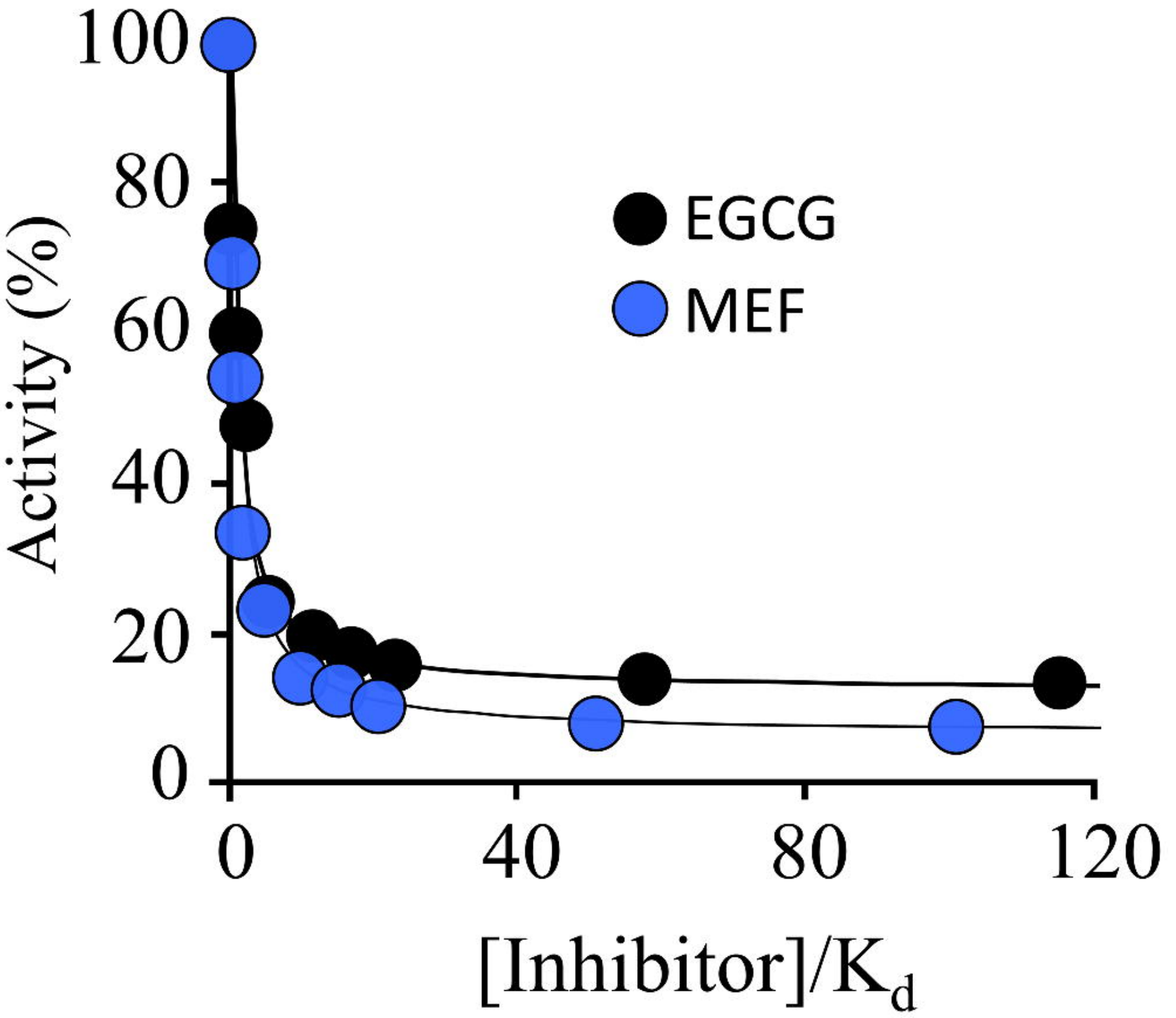

Figure 7.